

P2LSG: Powers-of-2 Low-Discrepancy Sequence Generator for Stochastic Computing

Mehran Shoushtari Moghadam , Sercan Aygun , Mohsen Riahi Alam , M. Hassan Najafi 

Abstract—Stochastic Computing (SC) is an unconventional computing paradigm processing data in the form of random bit-streams. The accuracy and energy efficiency of SC systems highly depend on the stochastic number generator (SNG) unit that converts the data from conventional binary to stochastic bit-streams. Recent work has shown significant improvement in the efficiency of SC systems by employing low-discrepancy (LD) sequences such as **Sobol** and **Halton** sequences in the SNG unit. Still, the usage of many well-known random sequences for SC remains unexplored. This work studies some new random sequences for potential application in SC. Our design space exploration proposes a promising random number generator for accurate and energy-efficient SC. We propose **P2LSG**, a low-cost and energy-efficient Low-discrepancy Sequence Generator derived from *Powers-of-2* VDC (Van der Corput) sequences. We evaluate the performance of our novel bit-stream generator for two SC image and video processing case studies: image scaling and scene merging. For the scene merging task, we propose a novel SC design for the first time. Our experimental results show higher accuracy and lower hardware cost and energy consumption compared to the state-of-the-art.

Index Terms—Emerging computing, image processing, low-discrepancy sequences, pseudo-random sequences, quasi-random sequences, stochastic computing, video processing.

I. INTRODUCTION

STOCHASTIC computing (SC) [1] is a re-emerging computing paradigm offering low-cost and noise-tolerant hardware designs. In contrast to traditional binary computing, which operates on positional binary radix numbers, SC designs process uniform bit-streams of ‘0’s and ‘1’s with no significant digits. While the paradigm was known for approximate computations for years, recent works showed deterministic and completely accurate computation using SC circuits [2], [3]. Encoding data from traditional binary to stochastic bit-streams is an important step in any SC system. The data are encoded by the probability of observing a ‘1’ in the bit-stream. For example, a bit-stream with 25% ‘1’ represents the data value of 0.25. The accuracy of the computations and the energy efficiency of the SC designs highly depend on this encoding step, particularly on the distribution of ‘1’s and ‘0’s in the bit-streams. A stochastic number generator (SNG), which encodes a data value in binary format to a stochastic bit-stream, consists of a random number generator (RNG) and a binary comparator. Fig. 1 shows the structure of an SNG commonly used in SC systems. At any cycle, the output of comparing the input data with the random number from the RNG unit produces one bit of the bit-stream.

The choice of the RNG unit directly affects the distribution of the bits in stochastic bit-streams. While traditionally *pseudo-random* sequences, generated by linear-feedback shift registers (LFSRs), were used in the SNG unit,

The authors are with the School of Computing and Informatics, Center for Advanced Computer Studies, University of Louisiana at Lafayette, Lafayette, LA 70503, USA (E-mail: {mehran.shoushtari-moghadam1, sercan.aygun, mohsen.riahi-alam, najafi}@louisiana.edu). This work was supported in part by National Science Foundation (NSF) grant #2019511, the Louisiana Board of Regents Support Fund #LEQSF(2020-23)-RD-A-26, and generous gifts from Cisco, Xilinx, and NVIDIA.

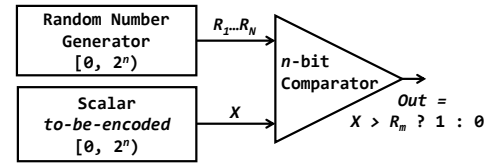


Fig. 1. The architecture of a stochastic number generator (SNG).

the state-of-the-art (SOTA) studies employ *quasi-random* sequences, such as **Sobol** (S) [4], [5] and **Halton** (HL) [6], [7] sequences, for high-quality generation of stochastic bit-streams. These sequences remove an important source of error in SC, the random fluctuation error [8] in generating bit-streams by producing *Low-Discrepancy* (LD) bit-streams. LD bit-streams quickly converge to the target value, reducing the length of bit-streams and, consequently, the latency of stochastic computations. This latency reduction directly translates to savings in energy consumption (i.e., power \times latency), a critical metric in the hardware efficiency of SC systems.

A challenge with the SOTA SNGs using sequences such as **Sobol** and **Halton** is their relatively high hardware cost that affects the achievable energy savings when using these sequences. This study extends the SOTA random sequences for the high-quality encoding of data in SC. We analyze some high-quality random sequences for possible improvement in the performance and hardware efficiency of the SNG unit. For the first time, to the best of our knowledge, we explore **Weyl** (W) [9], **R2** (R) [10], **Latin Hypercube** (L) [11], **Faure** (F) [12], **Hammersly** (HM) [13], **Niederreiter** (N) [14], [15], **Van der Corput** (VDC) [16], and **Poisson Disk** (P) [17] sequences in the context of SC as promising alternatives to prior costly LD sequences. The primary contributions of this work are summarized as follows:

- ① We employ some high-quality random sequences for the first time in SC literature. We evaluate the performance and accuracy of stochastic computations when using these sequences.
- ② We propose **P2LSG** (**P**owers-of-2 **L**ow-Discrepancy **S**equences **G**enerator), a lightweight LD Sequence Generator derived from *Powers-of-2* VDC sequences and evaluate its hardware cost compared to the SOTA.
- ③ For the first time, we introduce a novel SC video processing design for scene merging.
- ④ Experimental results on two SC image and video processing case studies show significant savings in area, energy, and latency with **P2LSG** compared to the SOTA non-parallel and parallel **Sobol**-based designs while maintaining comparative accuracy.

The rest of the paper is structured as follows. Section II provides the necessary background on random sequences and SC. Section III explores different random sequences in the context of SC. Section IV reveals the performance of **P2LSG** along with a new hardware design. Section V investigates the proposed generator for image scaling (interpolation) and scene merging. Finally, Section VI concludes the paper, summarizing the key findings and contributions.

II. BACKGROUND

A. Random Sequences

Random sequences are widely used in various research domains, particularly in emerging computing technologies [18]. Some sequences are binary-valued with logic-1s and logic-0s [19]. These sequences possess the orthogonality property; that is, different random sequences are (approximately) uncorrelated. Some sequences, on the other hand, are non-binary-valued (having fixed- or floating-point numbers). All non-binary-valued sequences listed in Section I (**S**, **HL**, **W**, **R**, **L**, **F**, **HM**, **N**, **VDC**, **P**) have LD properties. The *discrepancy* term in LD refers to how much the sequence points deviate from uniformity [20]. The *recurrence* property (i.e., the constructibility of further-indexed sequences from the previous-indexed ones) in LD sequences is beneficial for cross-correlation, which is advantageous for SC systems that require uncorrelated bit-streams [21].

The **Weyl** sequence belongs to the class of additive recurrence sequences, characterized by their generation through the iteration of multiples of an irrational number modulo 1. Specifically, by considering $\alpha \in \mathbb{R}$ as an irrational number and $x_i \in \{0, \alpha, 2\alpha, \dots, k\alpha\}$, the sequence $x_i - \lfloor x_i \rfloor$ (x_i modulo 1) produces an equidistributed sequence within the interval $(0, 1)$. Another example of an additive recurrence sequence is the **R** sequence, which is based on the *Plastic Constant* (the unique real solution of the cubic equation) [10], [22]. The **Latin Hypercube** sequences involve partitioning the sampling space into equally sized intervals and randomly selecting a point within each interval [23].

The **VDC** sequence serves as the foundation for many LD sequences. It is constructed by reversing the digits of the numbers in a specific base, representing each integer value as a fraction within the $[0, 1)$ interval. A **VDC** sequence in base- B is notated with **VDC-B**. As an example, the decimal value 11 in base-3 is represented by $(102)_3$. The corresponding value for the **VDC-3** is $2 \times 3^{-1} + 0 \times 3^{-2} + 1 \times 3^{-3} = \frac{19}{27}$. Similarly, the **Faure**, **Hammersley**, and **Halton** sequences are derived from the **VDC** concept using prime or co-prime numbers. To generate the **Faure** sequence in q -dimensions, the smallest prime number p is selected such that $p \geq q$. The first dimension of the **Faure** sequence corresponds to the **VDC-p** sequence, while the remaining dimensions involve permutations of the first dimension. The q -dimensional **Halton** sequence is generated by utilizing the **VDC** sequence with different prime bases starting from the first to the q -th prime number. A limitation of the **Halton** sequence is in utilizing prime number bases, which increases the complexity of the sequence generation [24].

The **Hammersley** sequence shares some similarities with the **Halton** sequence. For the sake of fair comparison with the **Halton** sequence we adopt different bases for the **Hammersley** sequence in this work. The first **Sobol** sequence is the same as the **VDC-2** sequence. The other **Sobol** sequence are generated through permutations of some sets of direction vectors [25]. The **Niederreiter** sequence is another variant of the **VDC** sequence relying on the powers of some prime numbers. This sequence features irreducible and primitive polynomials that ensure LD and uniformity over the sample space [26]. Finally, the **Poisson Disk** sequence generates evenly distributed numbers with minimal distance between them.

B. Stochastic Computing (SC)

SC has gained attention recently due to its intriguing advantages, such as robustness to noise, high parallelism, and low

design cost. Complex arithmetic operations are realized with simple logic gates in SC. Significant savings in the implementation costs are achieved for different applications, from image processing [27] to sorting [28], [29] and machine learning [30], [31], to name a few. Data conversion is an essential step in SC systems. Input numbers must be converted to random bit-streams, where each bit has equal significance. SC supports real data in the unit interval, i.e., $[0, 1]$. A common coding format is unipolar encoding (UPE). In UPE, the probability of observing a ‘1’ in the bit-stream X , i.e., $P(X = 1)$, equals the input value or x . The common method for generating a bit-stream of size N is to compare the input number with N random numbers ($R_1 \dots R_N$). This is usually done serially in N clock cycles. A logic-1 is produced at the output if the input value is greater than the random number; A logic-0 is produced otherwise. The distribution of logic-1s in the produced bit-stream depends on the sequence of random numbers. When dealing with the signed values (x is in the range $-1 \leq x \leq 1$), a bipolar encoding (BPE) is used, in which the probability that each bit in the bit-stream is ‘1’ is $P(X = 1) = \frac{(x+1)}{2}$.

SC operations consist of simple bit-wise logic operations. Multiplication of bit-streams in UPE is achieved by bit-wise AND [21], and in BPE by bit-wise XNOR operation [33]. For accurate multiplication, the input bit-streams must be *uncorrelated* with each other. Performing bit-wise AND on *correlated* bit-streams with a maximum overlap in the position of ‘1’s gives the *minimum* of the input bit-streams [28]. Scaled addition is realized in SC by a multiplexer (MUX) unit for both encodings [34]. For scaled subtraction, a MUX with one inverter is utilized [27]. The main inputs of the MUX can be correlated, but they should be uncorrelated with the select input bit-stream.

III. DESIGN SPACE EXPLORATION

This section comprehensively examines the use of the random sequences discussed in Section II for SC. We first analyze these sequences for basic SC operations and then extend the evaluations to more complex case studies. The numbers provided by these sequences are used as the required random numbers ($R_1 \dots R_N$) during bit-stream generation. Prior works used **Sobol** [4] and **Halton** [7] sequences for LD bit-stream generation. In this study, for the first time we propose **P2LSG**, a new LD sequence generator based on the **VDC Powers-of-2** bases (e.g., **VDC-2**, **VDC-4**, **VDC-8**, ..., **VDC-2^m ∈ Z⁺**) for cost-efficient LD bit-stream generation. The proposed sequence generator is cost- (area and power) and energy-efficient for hardware implementation.

A. Benchmark-I: SC Multiplication

We first evaluate the performance of the selected sequences for 2-input SC multiplication. Two input values (X_1 and X_2) are converted to bit-stream representation using random sequences, and the generated bit-streams are bit-wise ANDed to produce the output bit-stream. The resulting bit-stream is converted back to standard representation (by counting the number of ‘1’s and dividing by the length of the bit-stream) and compared with the expected multiplication result to find the absolute error. Here, the expected value is $P_{X_1} \times P_{X_2}$. For accurate multiplication, the input bit-streams must be *uncorrelated*. In the literature, *Stochastic Cross-Correlation (SCC)* is used to quantify the correlation between bit-streams [21]. In this metric, the correlation is calculated by using cumulative values denoted

TABLE I
MAE (%) COMPARISON OF USING DIFFERENT RANDOM SEQUENCES WHEN MULTIPLYING TWO 8-BIT PRECISION STOCHASTIC BIT-STREAMS WITH DIFFERENT BIT-STREAM LENGTHS.

Random Sequence	2 ⁶	2 ⁷	2 ⁸	2 ⁹	2 ¹⁰	2 ¹¹	2 ¹²	2 ¹³	2 ¹⁴	2 ¹⁵	2 ¹⁶
Sobol	0.92	0.45	0.19	0.092	0.041	0.019	0.009	0.0035	0.0013	0.0003	0.0000
R2	1.14	1.07	0.48	0.220	0.130	0.055	0.037	0.0164	0.0099	0.0078	0.0024
Weyl	1.46	1.40	0.83	0.530	0.400	0.220	0.190	0.1800	0.1300	0.0900	0.0065
Latin Hypercube	3.19	0.93	0.85	0.380	0.390	0.250	0.240	0.1200	0.0795	0.0508	0.0424
Faure	2.60	1.40	0.88	0.480	0.210	0.110	0.077	0.0360	0.0136	0.0113	0.0040
Halton	3.31	1.42	1.14	0.780	0.380	0.150	0.093	0.0570	0.0330	0.0150	0.0083
Hammersley	1.31	0.85	0.37	0.200	0.120	0.061	0.030	0.0170	0.0098	0.0043	0.0019
Niederreiter	0.95	0.51	0.34	0.130	0.072	0.032	0.019	0.0067	0.0039	0.0015	0.0011
Poisson Disk	4.16	2.61	1.06	0.960	0.710	0.340	0.440	0.3800	0.3700	0.6000	0.5200
P2LSG	1.76	0.88	0.39	0.170	0.073	0.030	0.012	0.0045	0.0015	0.0003	0.0000

The evaluation was conducted for 8-bit precision input data, and accurate multiplication results were obtained after $2^{2 \times 8}$ operation cycles. The assessment was performed for operation cycles ranging from 2^6 to 2^{16} , corresponding to bit-stream lengths varying from 2^6 to 2^{16} . In the experiment, the first two **Sobol** sequences were extracted from MATLAB. The π and *Silver Ratio* numbers were employed to generate the **Weyl** sequence. The **Faure** sequence was generated using **VDC-7**. The **Halton** sequence was utilized with **VDC-11** and **VDC-13**. The **Hammersley** sequence was constructed using **VDC-2** and **VDC-3**. For the **P2LSG** sequence, at each operation cycle i , the **VDC-2** and **VDC-2ⁱ** were employed. **Our framework can be found in [32].**

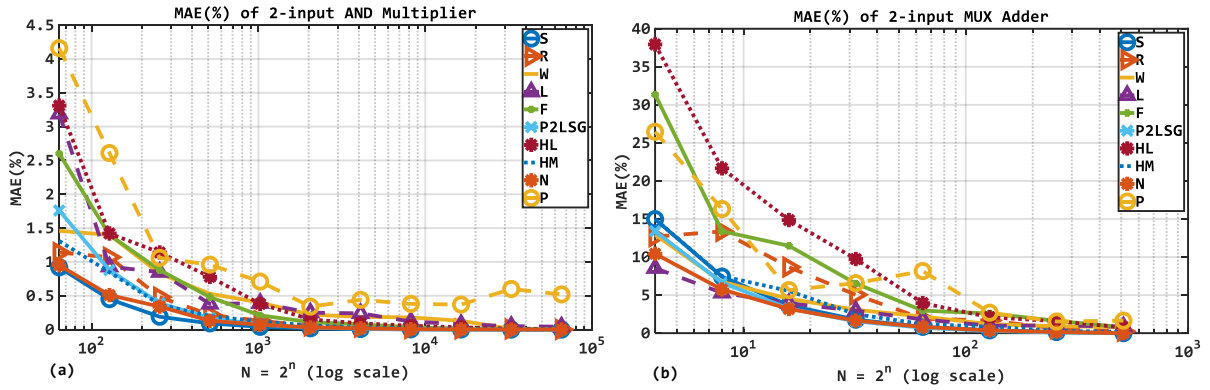


Fig. 2. MAE (%) of SC operation on two 8-bit precision input (a) SC Multiplication and (b) SC Scaled Addition. **VDC**-related sequences demonstrate favorable convergence rates. For approximate results, the **S**, **N**, **HM**, and **P2LSG** sequences emerge as the top performers.

TABLE II
MAE (%) COMPARISON OF THE TWO 8-BIT PRECISION INPUT BIT-STREAMS FOR SC SCALED ADDITION WITH DIFFERENT BIT-STREAM LENGTHS.

Seq.	2 ²	2 ³	2 ⁴	2 ⁵	2 ⁶	2 ⁷	2 ⁸	2 ⁹
Sobol	14.98	7.43	3.66	1.77	0.83	0.37	0.15	0.00
R2	12.69	13.37	8.68	5.04	1.91	1.66	0.60	0.25
Weyl	12.94	6.74	4.52	3.07	2.19	1.17	0.92	0.79
Latin Hypercube	8.54	5.30	3.92	2.95	1.81	0.97	1.02	0.86
Faure	31.35	13.39	11.48	6.52	2.96	2.59	1.62	0.78
Halton	37.94	21.66	14.86	9.74	3.95	2.09	1.58	0.75
Hammersley	14.98	7.49	5.55	2.49	1.19	0.85	0.29	0.18
Niederreiter	10.43	5.74	3.18	1.65	0.81	0.36	0.15	0.00
Poisson	26.46	16.31	5.66	6.57	8.16	2.69	1.53	1.65
P2LSG	13.40	6.63	3.24	1.55	0.71	0.29	0.097	0.00

For 8-bit precision input data, accurate scaled addition results were obtained after 2^{8+1} operation cycles. The evaluation was conducted for operation cycles ranging from 2^2 to 2^9 . In the experiment, the first two **Sobol** sequences were extracted from MATLAB. The π and *Silver Ratio* numbers were employed to generate the **Weyl** sequence. The **Faure** sequence was generated using **VDC-7**. The **Halton** sequence was utilized with **VDC-11** and **VDC-13**. The **Hammersley** sequence was constructed using **VDC-2** and **VDC-3**. For **P2LSG**, at each operation cycle i , the **VDC-2** and **VDC-2ⁱ** were employed.

by a , b , c , and d , which depend on the counts of 11, 10, 01, or 00 pairs in the overlapping bits between the two bit-streams:

$$SCC = \begin{cases} \frac{ad-bc}{N \times \min(a+b, a+c) - (a+b) \times (a+c)} & , \text{ if } ad > bc \\ \frac{ad-bc}{(a+b) \times (a+c) - N \times \max(a-d, 0)} & , \text{ else} \end{cases} \quad (1)$$

We exhaustively evaluated the multiplication accuracy for all cartesian combinations of $X1$ and $X2$ where the inputs are 8-bit precision values in the $[0, 1)$ interval (i.e., $\frac{0}{256}, \frac{1}{256}, \dots, \frac{255}{256}$). The bit-stream lengths vary from 2^6 to 2^{16} with $2 \times$ increments. Table I and Fig. 2 (a) present the Mean Absolute Error (MAE) of the multiplication results. We multiply the measured mean

values by 100 and report them as percentages. Two different sequences are selected for each case to satisfy the uncorrelation requirement ($SCC = 0$). For the **Sobol** sequence, the first two **Sobol** sequences from the MATLAB built-in **Sobol** sequence generator are used. For the **Faure** sequence, two sequences are created using **VDC-7**. The first dimension is generated using base-7, while the second is obtained through a permutation of the first one. The **Halton** sequence involves two dimensions generated using base-11 (**VDC-11**) and base-13 (**VDC-13**) with MATLAB built-in **Halton** function. For the **Hammersley** sequence, we use the **VDC-2** and **VDC-3** sequences. The **Latin Hypercube** sequence was also generated using its MATLAB built-in function. For the **Weyl** sequence, π and the *Silver Ratio* (i.e. $\sqrt{2} - 1$) were chosen as the irrational numbers. The first dimension of our **P2LSG** sequence is **VDC-2**, while **VDC-N** is selected for the other dimensions depending on the bit-stream length (N). As we move from left to right in Table I, the length of the bit-streams increases, and as expected, the accuracy improves (MAE decreases). Notably, the **VDC**-related sequences exhibit favorable convergence rates. Specifically, after 2^{10} operation cycles, the **P2LSG** sequence surpasses the **Niederreiter** sequence and approaches the **Sobol** sequence in terms of accuracy. For approximate results, the **Sobol**, **Niederreiter**, and **P2LSG** sequences emerge as the top performers. As can be seen in Fig. 2 (a), the convergence behavior of the **P2LSG** sequence outperforms other sequences as the length of the bit-stream increases.

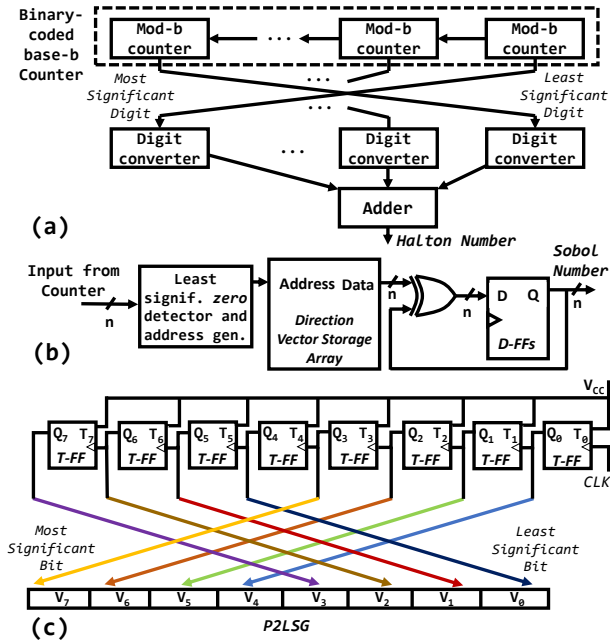


Fig. 3. (a) The **Halton** sequence generator implemented in [7], (b) The **Sobol** sequence generator proposed in [20], (c) Our proposed **P2LSG** design for base-16 (**P2LSG-16**) as an example; compared to SOTA designs of **Halton** and **Sobol** in (a) and (b), **P2LSG** utilizes only T-FFs and simple hard-wiring.

B. Benchmark-II: SC Addition

Next, we evaluate the accuracy of the SC *Scaled-Addition*. We utilize a 2-to-1 MUX with two 8-bit precision input operands similar to the multiplication operation. For this SC operation, the two addends (the main inputs of the MUX) are correlated ($SCC = 1$), while the MUX select input is uncorrelated to the addends [21]. To meet this requirement, we use a random sequence to generate the main input bit-streams and another sequence to generate the bit-stream corresponding to the MUX select input. For two-input addition, a bit-stream corresponding to 0.5 value is generated for the select input. Table II and Fig. 2 (b) present the accuracy results in terms of MAE for different bit-stream lengths. Due to using a select input with 2-bit precision (i.e., 0.5 value), accurate output (0.0% MAE) can be achieved with a bit-stream length of 2^9 by using sequences such as **Sobol**, **Niederreiter**, **Hammersley**, and **P2LSG**. As can be seen in Table II, for bit-stream sizes greater than 2^4 , the **P2LSG** sequence achieves the minimum MAE among the other sequences. By increasing the bit-stream length (N), we can see that the MAE tends to zero for **Sobol** and **P2LSG** sequences.

IV. PROPOSED SEQUENCE GENERATOR

In this section, we propose a novel hardware design for **P2LSG** and evaluate its implementation cost compared to prior LD sequence generators. Alaghi and Hayes [7] implemented a **Halton** sequence generator consisting of mod counters, digit converters, and an adder. Fig. 3 (a) shows the **Halton** generator of [7]. Liu and Han [20] proposed a **Sobol** sequence generator by using some Direction Vectors (DVs). The DVs ($V_x(x = 0, 1, \dots, N - 1)$) are generated using some primitive polynomials and stored in a Direction Vector Array (DVA). By employing different DVs, different **Sobol** sequences can be produced. In their design, a priority encoder finds the least significant zero (LSZ) in the output of a counter at any cycle. Depending on the position of the LSZ, a DV is selected from

the DVA. A new **Sobol** number is recursively generated by XORing the respective DV and the previous **Sobol** number. Fig. 3 (b) shows the design of this **Sobol** generator.

Prior work suggested a look-up table-based approach for generating **VDC** sequences [35] without a custom hardware design for SC bit-stream generation. We propose a low-cost design for efficient and lightweight generation of the **P2LSG** sequences. Our design uses a $\log_2(N)$ -bit counter for generating different sequences of *Powers-of-2* bases up to N , where N is the length of the bit-stream.

For a fair comparison with previous random generators and to assess the performance for various image processing applications, we target bit-streams of up to 256 (sufficient for representing 8-bit grayscale image data). Therefore, we require up to 256 different random numbers from the sequence generator to generate each bit-stream. The general algorithm to generate a base-B **VDC** sequence consists of five steps:

- 1 Generating an integer number.
- 2 Converting the integer number to its base-B representation.
- 3 Reversing the base-B representation.
- 4 Converting the base-B representation to a binary number.
- 5 Scaling the input number within the $[0, 1)$ interval to the corresponding 8-bit binary number in the $[0, 256)$ range to be connected to the binary comparator.

The complexity of the hardware design for this algorithm is closely tied to the chosen base. We classify the hardware designs into two categories depending on the selected base: *Class-I*: those *without Powers-of-2* bases, and *Class-II*: those *with Powers-of-2* bases.

A. Class-I: Non-Powers-of-2 Base Generators

To implement this type of **VDC** sequence generators, we combine the first two steps, 1 and 2, by utilizing a base-B counter to generate the integer numbers in the corresponding base. For instance, a *Binary Coded Decimal* (BCD) counter can be employed for a base-10 representation. Step 3 is achieved by hard-wiring. Step 4 is implemented by employing adders and MUXs. This step is relatively complex and takes more hardware resources compared to the other steps. Step 5 can simply be achieved by shift operations.

The **Hammersley** and **Halton** sequences extend the **VDC** sequence to higher dimensions, representing each dimension in a different prime base-B. Consequently, the hardware implementation of these sequences falls under this particular type of sequence generator. The need for counters with prime radices and base conversion make the **Halton** sequence generator of [7] complex to implement in hardware. The hardware limitations of the design of [7] motivate us to explore the second class of generators for the *Powers-of-2* bases that build **P2LSG**.

B. Class-II: Powers-of-2 Base Generators

1) *Sequential Design*: To implement *Powers-of-2* base generators, a binary counter with sufficient bits is utilized to represent the desired range of integer numbers in step 1. To convert the value of a binary counter to its base-B representation (step 2), we consider groups of $\log_2(B)$ bits, starting from the least significant bit. If the last group lacks enough bits, some additional '0' bits are appended via zero padding to ensure it forms a complete group. The reversing operation in step 3 is done by hard-wiring each group of bits, treating them as a single digit in base-B. The process of converting a base-B number to its equivalent binary representation is the inverse of

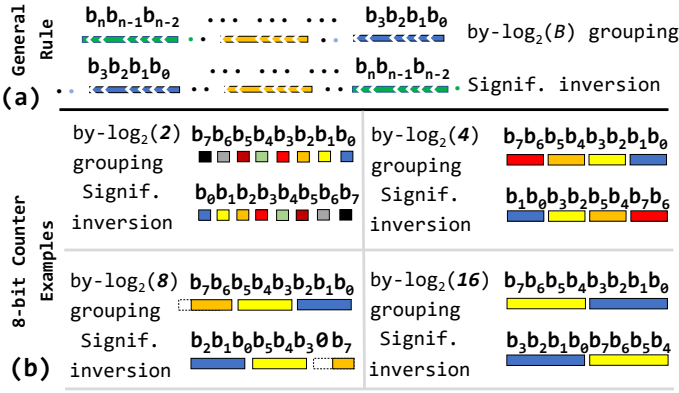


Fig. 4. Proposed **P2LSG**. (a) The general rule to hard-wiring bits for reversing operation (aka., significance inversion), and (b) Example for the 8-bit counter to generate **P2LSG-2**, **P2LSG-4**, **P2LSG-8**, and **P2LSG-16** sequences (up to **P2LSG-256** is possible).

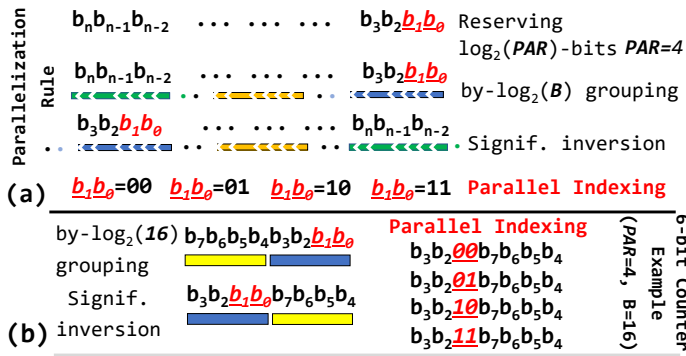


Fig. 5. Parallel **P2LSG** sequence generator. (a) The general rule to assign parallel indexing bits, and (b) **P2LSG-16** example with $PAR = 4$ concurrent sequence generation.

step 2. In this process, each group or base- B digit is considered as equivalent $\log_2(B)$ bits of binary representation and any exceeding bits beyond the counter in step 1 is discarded. Fig. 3 (c) demonstrates a simple 8-bit precision **P2LSG** for base-16 (**P2LSG-16**).

An Up-Counter counts up to 255, and the target sequence is obtained by significance inversion of each group; the least significant group becomes the most significant group, and vice versa. For this base-16 example, the output Q_3 of the 4th T Flip-Flop (T-FF) from the right side becomes the most-significant bit. Fig. 4 (a) shows the overall idea behind the proposed **P2LSG**. After grouping each bit from the counter, the inversion (via hard-wiring) reverses the bit significance; the new binary output is ready for comparison in the SNG block. Fig. 4 (b) illustrates examples of different bases.

TABLE III
HARDWARE COST COMPARISON FOR GENERATING TWO DIFFERENT 8-BIT RANDOM SEQUENCES.

SNG	Area (μm^2)	Power (μW)	CPL (ns)
Sobol#2 & Sobol#3 [5]	2×781	2×45.15	0.68
Halton#1 & Halton#2	$130 + 450$	$15.15 + 35.30$	1.06
P2LSG-4 & P2LSG-16	163	16.05	0.49

Halton#1 and Halton#2 are generated using VDC-2 and VDC-3, respectively. In this case, the base-2 and base-3 counters are utilized to generate the Halton sequence. It is worth noting that designing counters with prime bases (except base-2) can lead to a significant hardware cost. As for **P2LSG-4** and **P2LSG-16**, they employ VDC-4 and VDC-16, respectively. Any Powers-of-2 bases can be utilized to generate **P2LSG** sequences with the similar design in Fig. 3 except with different hard-wiring schemes. (CPL: Critical Path Latency)

2) *Parallel Design*: Our proposed *Class-II P2LSG* can also operate in parallel. Fig. 5 illustrates how more than one number of a **P2LSG** sequence (in any base) can be generated in parallel at any cycle. Let us define PAR as the number of sequence elements to be generated in parallel. First, $\log_2(PAR)$ bits are reserved at the least significant positions. The remaining bits require a reduced precision counter (e.g., $8 \rightarrow 6$ in Fig. 5). At any clock cycle, the reserved bits are filled with $2^{\log_2(PAR)}$ possible logic values (parallel indexing). Fig. 5 (a) shows an example for $PAR = 4$. In this example, each output repeats four times to fill the reserved bits with 00, 01, 10, and 11. The outputs at any cycle produce four consecutive numbers. Fig. 5 (b) illustrates another example of $PAR = 4$ for **P2LSG-16**.

Table III compares the hardware cost of generating Sobol and Halton sequences with the proposed sequence generator. We report the hardware area, power consumption, and critical path latency (CPL) for each case. We synthesized the designs using the Synopsys Design Compiler v2018.06 with the 45nm FreePDK gate library [36]. The reported numbers in Table III demonstrate that the proposed sequence generator surpasses the Sobol and Halton sequence generators in terms of hardware efficiency.

V. SC IMAGE AND VIDEO CASE STUDIES

In this section, we evaluate the performance and the hardware efficiency of the proposed **P2LSG** in two SC image and video processing case studies. Prior work has used SC for low-cost implementation of different computer vision tasks from depth perception to interpolation [27], [37]–[41]. We first evaluate the proposed sequence generator in an interpolation and image scaling application and then implement and study its effectiveness in a novel SC circuit for scene merging video processing, which we propose for the first time in the literature.

A. Interpolation and Image Scaling

Interpolation refers to the process of estimating or calculating values between two known data points. Linear interpolation is a method used to estimate values between two known values based on a linear relationship [42]. It assumes a straight line between the available values and calculates intermediate values along that line. In image processing, linear interpolation is used to estimate pixel values between two neighbouring pixels. It is commonly employed when performing operations such as rotation, translation, or affine transformations on images. Bilinear interpolation is a specific case of linear interpolation applied in two dimensions. Instead of estimating values along a straight line, it estimates values within a two-dimensional grid of pixels [43]. Bilinear interpolation considers the four nearest pixels to the target location and calculates a weighted average based on their values. The weights are determined by the distances between the target location and the surrounding pixels; thereby, an image scaling task can be performed [44].

Assume we have an original image, I , with pixel values represented by a 2-D array. We want to estimate the pixel value at a non-integer coordinate (x, y) in the image. The four surrounding pixels to consider are (x_1, y_1) , (x_1, y_2) , (x_2, y_1) , and (x_2, y_2) , where (x_1, y_1) represents the pixel at the bottom-left corner of the target location, and (x_2, y_2) represents the pixel at the top-right corner. Let us denote the pixel values as $I(x, y)$, $I(x_1, y_1)$, $I(x_1, y_2)$, $I(x_2, y_1)$, and $I(x_2, y_2)$. The bilinear interpolation formula to estimate the pixel value $I(x, y)$ is as follows: $I(x, y) = (1 - u)(1 - v) \times I(x_1, y_1) + (1 - u)v \times$

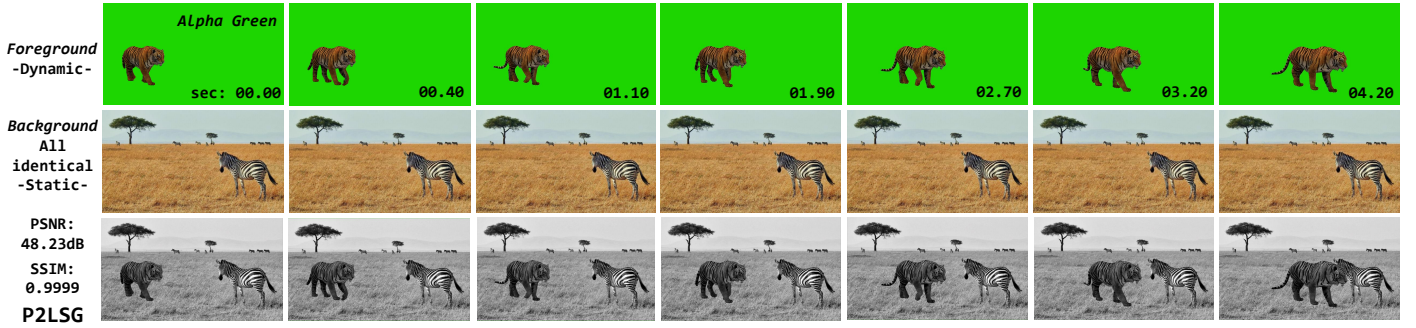


Fig. 6. SC-based video processing for scene merging. The foreground video with green background is embedded into a static jungle background picture. The figure shows several frames from the first 04.20 sec of the video in the test. For $N=256$, the results of **P2LSG**-based and **Sobol**-based SC designs alongside the reference binary-based conventional processing can be accessed from: https://github.com/mehranUL/LD_Seqs_SC/blob/main/Processed_videos/.

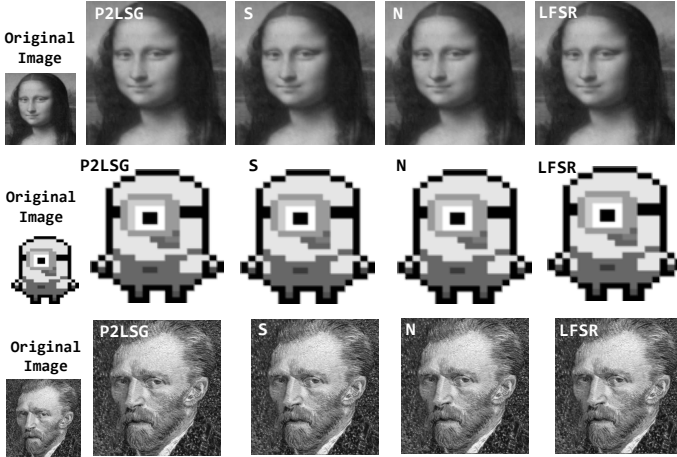


Fig. 7. Visual results of SC image scaling using different SNGs (with **P2LSG**, **Sobol**, **Niederreiter**, or **LFSR**) and a 4-to-1 MUX.

TABLE IV
SC IMAGE SCALING WITH DIFFERENT RANDOM SEQUENCES.

Image Scaling (<i>Scale Factor=2</i>)			
P2LSG	Sobol (S)	Niederreiter (N)	LFSR
<i>Mona Lisa</i>			
PSNR: 46.62dB SSIM: 0.9958	PSNR: 46.25dB SSIM: 0.9948	PSNR: 46.37dB SSIM: 0.9949	PSNR: 44.63dB SSIM: 0.9892
<i>Minion</i>			
PSNR: 39.36dB SSIM: 0.9975	PSNR: 39.26dB SSIM: 0.9926	PSNR: 39.30dB SSIM: 0.9958	PSNR: 38.50dB SSIM: 0.9964
<i>Van Gogh</i>			
PSNR: 43.10dB SSIM: 0.9958	PSNR: 42.91dB SSIM: 0.9921	PSNR: 42.99dB SSIM: 0.9923	PSNR: 41.65dB SSIM: 0.9880

$I(x_1, y_2) + u(1-v) \times I(x_2, y_1) + uv \times I(x_2, y_2)$, where $u = x - x_1$ (fractional distance between x and x_1) and $v = y - y_1$ (fractional distance between y and y_1). The values $(1-u)(1-v)$, $(1-u)v$, $u(1-v)$, and uv are the weights assigned to each surrounding pixel. These weights represent the contribution of each pixel to the interpolated value. The interpolation formula can be compared to a multiplication-based SC MUX structure [34], where neighbouring pixels are fed into the main MUX inputs, and the location information is fed into the selection ports. In this scenario, a 4-to-1 MUX can be expressed in terms of probabilities as follows: $P_{I(x,y)} = (1 - P_u)(1 - P_v)P_{I_{11}} + (1 - P_u)(P_v)P_{I_{12}} + (P_u)(1 - P_v)P_{I_{21}} + (P_u)(P_v)P_{I_{22}}$.

Fig. 7 visually demonstrates the outputs of $2\times$ image scaling with an SC circuit composed of SNGs for data conversion and a 4-to-1 MUX unit. Table IV presents the performance results in terms of peak-signal-to-noise ratio (PSNR) and structural

TABLE V
HARDWARE COST COMPARISON OF THE IMAGE AND VIDEO PROCESSING CASE STUDIES.

$N=256$	Area (μm^2)	*Energy (pJ)	*CPL (ns)	Total Energy (μJ)	Runtime
Image Scaling					
Sobol [5]	2017	17.55	366	0.781	16.3 ms
Parallel $4\times$ Sobol	4548	16	91.5	0.713	4.07 ms
P2LSG	715	5.6	317	0.25	14.12 ms
Parallel $4\times$ P2LSG	2040	2.4	71	0.107	3.16 ms
Scene Merging					
Sobol [5]	1787	16.6	353	1568	33.3 s
Parallel $4\times$ Sobol	3628	15.1	88	1424	8.33 s
P2LSG	485	4.7	304	443	28.7 s
Parallel $4\times$ P2LSG	1120	1.48	68	140	6.4 s

*Energy and *CPL are for producing each output pixel. Bit-stream Length (N) is 256. (CPL: Critical Path Latency)

similarity (SSIM). We evaluated the SC circuit for the cases of using the **P2LSG**, **Sobol (S)**, **Niederreiter (N)**, and **LFSR** random sequences in the SNG units. We processed the *Mona Lisa*, *Minion*, and *Van Gogh* images as the test images. The results shown in Fig. 7 and Table IV show the superior performance of the **P2LSG** sequences. We further evaluated the performance and energy consumption in 45nm CMOS technology when processing the *Mona Lisa* image (107×104 image size) for the two cases of **P2LSG** and **Sobol**. Table V reports the results. As reported, the non-parallel and the $4\times$ parallel designs of the **P2LSG**-based implementation save area by 64% and 55%, energy by 67% and 85%, and CPL by 13% and 22% compared to the non-parallel and $4\times$ parallel **Sobol**-based implementation, respectively.

B. SC Video Processing: Scene Merging

As the second case study, we introduce an SC circuit for scene merging in video processing. The goal is to merge two different scenes in a video. One scene is a static image (background), while the other is a moving video sequence (foreground). To composite the images, the background image is processed with a transparent foreground image (green *alpha* channel) using the formula: $\text{Merged Pixel} = \text{Background Pixel} \times (1 - \alpha) + \text{Foreground Pixel} \times \alpha$ [45]. Here, the *alpha* channel, which depends on the dynamic movement of the moving object in the green background of the video, is updated frame by frame. Considering that the *alpha* value should be within the $[0, 1]$ interval, the formula can be seen as a MUX with inputs being the foreground and background scenes and the selection port being the *alpha* channel: $\text{MUX} = P_{X_1}(1 - P_S) + P_{X_2}P_S$, where P_{X_1} and P_{X_2} are the circuit inputs and P_S is the select

input [34]. Based on this analogy, the provided video in Fig. 6, which features a moving tiger, is merged with an African jungle background. Using the **P2LSG** sequence for data conversion and a 2-to-1 MUX as the SC circuit, the processed video achieves a PSNR of 48.23dB and an SSIM of 0.999. The video has a duration of 6.06 seconds and was generated at a frame rate of 30 frames per second. We also achieved similar PSNR and SSIM values (48.13dB and 0.9999) when using the **Sobo1**-based SNG for data conversion. As the hardware results presented in Table V demonstrate, the non-parallel and 4× parallel **P2LSG** design provide 73% and 69% lower area, 72% and 90% lower energy consumption, and 14% and 23% lower runtime compared to the non-parallel and 4× parallel **Sobo1**-based design.

VI. CONCLUSIONS

This study explores new design possibilities for SC by analyzing some well-known random sequences in the literature. As a promising random sequence for the SNG unit of SC systems, we evaluated the performance of the Powers-of-2 Low-Discrepancy Sequence Generator (**P2LSG**) sequences. We proposed a lightweight hardware design for **P2LSG** sequence generation. The proposed generator provides a higher hardware efficiency compared to the SOTA LD sequence generators. We evaluated the performance of the **P2LSG**-based SNGs in an image scaling and a scene merging video processing case study. Our performance evaluation and hardware cost comparison show comparable or better numbers compared to the SOTA. Our finding opens possibilities for incorporating the **P2LSG** sequences in other emerging paradigms that require orthogonal vectors, such as hyperdimensional computing. The **P2LSG** sequences can be utilized to address the computational needs and improve the performance of such paradigms. We leave studying this aspect for our future work.

REFERENCES

- [1] B. R. Gaines, *Stochastic Computing Systems*. Boston, MA: Springer US, 1969, pp. 37–172. [Online]. Available: https://doi.org/10.1007/978-1-4899-5841-9_2
- [2] M. H. Najafi, D. J. Lilja, and M. D. Riedel, “Performing stochastic computation deterministically,” *IEEE TVLSI*, vol. 27, no. 12, pp. 2925–2938, 2019.
- [3] M. Riahi Alam, M. H. Najafi, and N. TaheriNejad, “Exact stochastic computing multiplication in memristive memory,” *IEEE Design & Test*, vol. 38, no. 6, pp. 36–43, 2021.
- [4] S. Liu and J. Han, “Energy efficient stochastic computing with sobol sequences,” in *2017 DATE*, 2017, pp. 650–653.
- [5] M. H. Najafi, D. J. Lilja, and M. Riedel, “Deterministic methods for stochastic computing using low-discrepancy sequences,” in *2018 ICCAD*, 2018, p. 1–8.
- [6] Z. Lin, G. Xie, W. Xu, J. Han, and Y. Zhang, “Accelerating stochastic computing using deterministic halton sequences,” *IEEE TCAS II*, vol. 68, no. 10, pp. 3351–3355, 2021.
- [7] A. Alaghi and J. P. Hayes, “Fast and accurate computation using stochastic circuits,” in *DATE*, 2014, pp. 1–4.
- [8] P. Ting and J. P. Hayes, “Eliminating a hidden error source in stochastic circuits,” in *2017 IEEE DFT*, 2017, pp. 1–6.
- [9] H. V. Weyl, “Über die gleichverteilung von zahlen mod. eins,” *Mathematische Annalen*, vol. 77, pp. 313–352, 1916.
- [10] “Unreasonable Effectiveness of Quasirandom Sequences,” <https://extremelarning.com.au/unreasonable-effectiveness-of-quasirandom-sequences/>, [Accessed 10-May-2023].
- [11] M. D. McKay, R. J. Beckman, and W. J. Conover, “Comparison the three methods for selecting values of input variable in the analysis of output from a computer code,” *Technometrics; (United States)*, vol. 21:2, 5 1979. [Online]. Available: <https://www.osti.gov/biblio/5236110>
- [12] H. Faure, “Variations on (0, s)-sequences,” *Journal of Complexity*, vol. 17, no. 4, p. 741–753, Dec 2001.
- [13] J. M. Hammersley and D. C. Handscomb, *Monte Carlo Methods*. Springer Netherlands, 1964. [Online]. Available: <http://dx.doi.org/10.1007/978-94-009-5819-7>
- [14] L. Kuipers and H. Niederreiter, *Uniform Distribution of Sequences*, ser. Dover Books on Mathematics. Mineola, NY: Dover Publ., 2006.
- [15] H. Niederreiter and C. Xing, “Low-discrepancy sequences and global function fields with many rational places,” *Finite Fields and Their Applications*, vol. 2, no. 3, pp. 241–273, 1996.
- [16] J. G. van der Corput, “Verteilungsfunktionen. I,” *Proc. Akad. Wet. Amsterdam*, vol. 38, pp. 813–821, 1935.
- [17] R. L. Cook, “Stochastic sampling in computer graphics,” *ACM Trans. Graph.*, vol. 5, pp. 51–72, 1988.
- [18] S. Aygun, M. S. Moghadam, M. H. Najafi, and M. Imani, “Learning from hypervectors: A survey on hypervector encoding,” 2023, arXiv:2308.00685. [Online]. Available: <https://arxiv.org/abs/2308.00685>
- [19] A. Mitra, “On pseudo-random and orthogonal binary spreading sequences,” *Int. J. of El. and Comm. Eng.*, vol. 2, no. 12, pp. 2836–2843, 2008.
- [20] S. Liu and J. Han, “Toward energy-efficient stochastic circuits using parallel sobol sequences,” *IEEE TVLSI*, vol. 26, no. 7, 2018.
- [21] A. Alaghi and J. P. Hayes, “Exploiting correlation in stochastic circuit design,” in *ICCD*, Asheville, NC, USA, 2013, pp. 39–46.
- [22] L. Marohnic and T. Strmevcki, in *Plastic Number: Construction and Applications*, 2012.
- [23] C. D. Lin and B. Tang, “Latin hypercubes and space-filling designs,” 2022.
- [24] I. Krykova, “Evaluating of path-dependent securities with low discrepancy methods,” Master’s thesis, Worcester Polytechnic Institute, January 2004.
- [25] I. L. Dalal, J. Harwayne-Gidansky, and D. Stefan, “Low discrepancy sequences for monte carlo simulations on reconfigurable platforms,” in *ASAP*, 2008, pp. 108–113.
- [26] R. Lidl and H. Niederreiter, *Finite Fields*, ser. EBL-Schweitzer. Cambridge University Press, 1997, no. v. 20, pt. 1. [Online]. Available: <https://books.google.com/books?id=xqMqxQTFUKMC>
- [27] P. Li, D. J. Lilja, W. Qian, K. Bazargan, and M. D. Riedel, “Computation on stochastic bit streams digital image processing case studies,” *IEEE TVLSI*, vol. 22, no. 3, 2014.
- [28] M. H. Najafi, D. J. Lilja, M. D. Riedel, and K. Bazargan, “Low-cost sorting network circuits using unary processing,” *IEEE TVLSI*, vol. 26, no. 8, pp. 1471–1480, 2018.
- [29] M. H. Najafi, “New views for stochastic computing: From time-encoding to deterministic processing,” Ph.D. dissertation, University of Minnesota, Minneapolis, USA, 2018.
- [30] Z. Li, J. Li, A. Ren, R. Cai, C. Ding, X. Qian, J. Draper, B. Yuan, J. Tang, Q. Qiu, and Y. Wang, “Heif: Highly efficient stochastic computing-based inference framework for deep neural networks,” *IEEE TCAD*, vol. 38, no. 8, pp. 1543–1556, 2019.
- [31] S. Aygun, “Stochastic bitstream-based vision and learning machines,” Ph.D. dissertation, Istanbul Technical University, Istanbul, Turkey, 2022.
- [32] “Github,” https://github.com/mehranUL/LD_Seqs_SC, 2023.
- [33] J. Li, Z. Yuan, Z. Li, C. Ding, A. Ren, Q. Qiu, J. Draper, and Y. Wang, “Hardware-driven nonlinear activation for stochastic computing based deep convolutional neural networks,” in *IJCNN*, Anchorage, AK, USA, 2017, pp. 1230–1236.
- [34] T. J. Baker and J. P. Hayes, “Cemux: Maximizing the accuracy of stochastic mux adders and an application to filter design,” *ACM Trans. Des. Autom. Electron. Syst.*, vol. 27, no. 3, jan 2022.
- [35] V. T. Lee, “Towards practical stochastic computing architectures for emerging applications,” Ph.D. dissertation, Uni. of Washington, USA, 2019. [Online]. Available: <http://hdl.handle.net/1773/43658>
- [36] “FreePDK 45nm Library,” <https://github.com/mflowgen/freepdk-45nm/>, [Accessed September 10, 2023].
- [37] W. Qian, X. Li, M. D. Riedel, K. Bazargan, and D. J. Lilja, “An Architecture for Fault-Tolerant Computation with Stochastic Logic,” *Computers, IEEE Trans. on*, vol. 60, no. 1, pp. 93–105, Jan 2011.
- [38] Y. Hu, T. Zhang, R. Wei, M. Li, R. Wang, Y. Wang, and R. Huang, “Accurate yet efficient stochastic computing neural acceleration with high precision residual fusion,” in *DATE*, 2023, pp. 1–6.
- [39] R. Wang, J. Han, B. F. Cockburn, and D. G. Elliott, “Stochastic circuit design and performance evaluation of vector quantization for different error measures,” *IEEE TVLSI*, vol. 24, no. 10, pp. 3169–3183, 2016.
- [40] M. H. Najafi and D. J. Lilja, “High-speed stochastic circuits using synchronous analog pulses,” in *ASP-DAC*, 2017, pp. 481–487.
- [41] S. Aygün, M. Altun, and E. O. Güneş, “Sobel filter operation in image processing via stochastic arithmetic-logic unit design,” in *2017 IEEE SIU*, 2017.
- [42] T. Blu, P. Thevenaz, and M. Unser, “Linear interpolation revitalized,” *IEEE Transactions on Image Processing*, vol. 13, no. 5, pp. 710–719, 2004.
- [43] K. Gribbon and D. Bailey, “A novel approach to real-time bilinear interpolation,” in *DELTA*, 2004, pp. 126–131.
- [44] W. H. Press, S. A. Teukolsky, W. T. Vetterling, and B. P. Flannery, *Numerical Recipes in C: The Art of Scientific Computing*. New York, NY, USA: Camb. Univ. Press, 1995.
- [45] Y. Sun, C.-K. Tang, and Y.-W. Tai, “Semantic image matting,” in *IEEE/CVF CVPR*, June 2021, pp. 11 120–11 129.